Signal Preprocessing Methods for Automated Analysis of Eddy Current Signatures during Manual Inspection

Adam DOČEKAL, Marcel KREIDL, Radislav ŠMÍD
Department of Measurement, Faculty of Electrical Engineering,
Czech Technical University, Prague, Czech Republic

Abstract. In this contribution, a novel method for the automatic evaluation of flaws during a manual Eddy Current (EC) inspection procedure is presented. Algorithms were especially designed with respect to characteristics typical for a hand-held EC testing procedure. In manual scanning, a signal related to impedance change in the complex plane is affected by large and unpredictable variations of scanning speed and alternations of the probe position. The detection of flaws in the object tested is also affected by the imperfections of device electronics, mainly of null drift. The lift-off effect of the inspection probe is required for consideration as well.
This contribution describes an algorithm implementing an event detection method for event detection in a complex eddy current signal insensitive to some of the effects listed above. The paper mainly introduces a robust EC signal normalization procedure using non-linear filtration based on the evaluation of the distance between consecutive samples in the complex plane and median based tracking of the EC signature.
A normalized EC signature was used to classify flaws in a tested object. A feature extraction was performed using Modified Fourier coefficients. The classification was performed by using three different methods: nearest-mean classifier, k-nearest neighbourhood classifier and back-propagation neural network.
The methods were tested on a single frequency instrument with an absolute probe.

Introduction

Methods based on Eddy Current (EC) inspection have become one of the most widely used and trusted techniques for non-destructive crack detection in steam generator tubes in nuclear power plants and in aircraft maintenance, where a typical task consists of the inspection for cracks beneath rivets in layered structures. Conventional Eddy current techniques use single frequency sinusoidal excitation and detect flaws as impedance or voltage changes on an impedance plane display with inspectors interpreting the magnitude and phase changes. The trajectory in the complex plane, the EC signature, is usually described in automated analysis systems. The complex signal $\boldsymbol{s}(n)$ is represented by the horizontal component $h(n)$ and the vertical component $v(n)$, see equation (1).

$$\boldsymbol{s}(n) = h(n) + \mathrm{i}\, v(n) \tag{1}$$

However, these techniques are sensitive to a variety of parameters that are inherent in the flaws, e.g. lift-off and signal anomalies caused by the set-up of the object to be tested. Furthermore, multiple frequency measurements have been combined to provide a more rigorous assessment of structural integrity by reducing signal anomalies that may otherwise

mask the flaws, but some adverse effects, e.g. lift-off, could be suppressed even if a single frequency instrument is used for testing.

Eddy current sensors are generally robust and small in size. Because the EC testing does not require additional cleaning or another surface treatment, non-contact eddy sensors and appropriate testers are often used as a small and portable man-held device. During manual inspection, a visual interpretation is usually used for eddy current data analysis. This method requires highly trained personnel, the results are influenced by the subjectivity of human perception, and the inspection procedure is relatively slow. Therefore, an automated evaluation of EC signals is very desirable.

Unlike automated scanning (robotic) systems equipped with precise motorized EC probe positioning, manual inspections are essential for testing complicated structures and surfaces. During manual scanning, the EC signal quality could be dramatically degraded by variations in the scanning speed and alternations of the probe to surface position, e.g. tilt or lift-off. In this paper, a robust normalization procedure for processing EC signals is described, taking into account manual scanning features and a method for feature extraction based on Fourier or Wavelet transformation. These methods are verified by testing samples and the classification of the obtained features. Commonly known classifiers are used for this purpose: nearest-mean classifier, k-nearest neighbourhood classifier, and back-propagation neural network. The use of further non-linear classification methods for this purpose i:

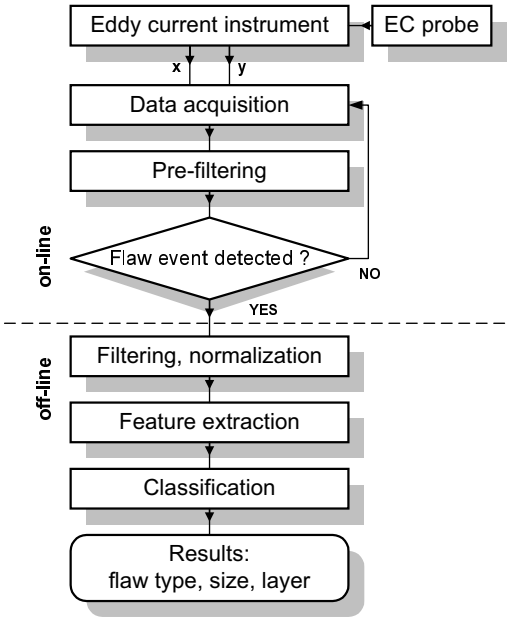

Fig. 1. Block diagram of EC inspection system with automated analysis of the EC signal

2. Data Acquisition and Event Detection

The scheme of the EC inspection system with an automated analysis of the EC signal is shown in Fig. 1. The EC signals from portable NDT instruments were digitized by a 2-channel 12-bit analogue-to-digital converter (ADC) at a sampling frequency of 10 kHz to obtain a discrete complex signal. The real-time data stream $\boldsymbol{s}(n)$ is captured in a FIFO circular buffer to ensure independency of the signal analysis to the asynchronous operation of the ADC. This circular buffer is formed from the linear FIFO memory structure by re-indexing. The further processing can be divided into two blocks.

In the first block, the data are processed on-line and the signal segments containing possible flaw signatures are detected. To ensure impulse noise suppression, the signal is non-linearly filtered by a simple median filter length L_w using a window moved continuously with incoming data. The offset of the raw signal is eliminated by subtraction of the initial value that is obtained during nulling (calibrating) the EC instrument.

Drift arising in the EC probe and instrument mainly due to temperature dependency can be cancelled using the simplified LMS predictive algorithm. Especially for testing with man-held probes, this algorithm also partially suppresses the influence of the EC probe hold manner. Using the described algorithm supposes pretty linear (predictable) behaviour of the drift. Flaw event detection is based on the evaluation of the signal amplitude $m(n)$ of the filtered complex EC signal $\mathbf{s}(n)$.

$$m(n) = \sqrt{h(n)^2 + v(n)^2} \tag{2}$$

Flaw detection and drift cancellation can be performed in a single procedure described as follows. First, the estimation error of the actual value prediction is calculated as:

$$e(i) = w(i) - a(i), \tag{3}$$

where $w(i)$ is the median value of $m(n)$ for $i \cdot L_w < n \le (i+1) \cdot L_w$. The new estimation $a(i)$ is computed as:

$$a(i) = a(i-1) + \alpha \cdot e(i), \tag{4}$$

where α is a constant related to the maximum drift of the signal. The algorithm is initialized with $a(1) = w(1)$. The EC event (possible flaw) is detected if the estimation error $e(i)$ is greater than a selected threshold value e_t and the appropriate section of the signal is stored for further analysis.

The signal segment containing the flaw event is processed off-line in the second block. This block is described in the following sections.

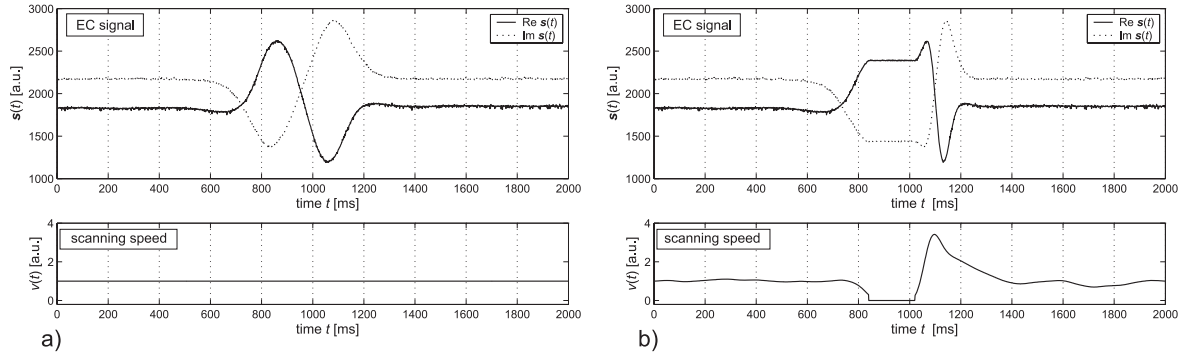

Fig. 2. Signal from EC probe for: a – motorized positioning, b – manual scanning by human operator. The same instrument and setup were used. The flaw width on surface was 0.3 mm.

3. Signal Normalization

The important problem in automated EC signal evaluation during manual EC inspection is large and unpredictable variations of the scanning speed. Methods that do not take this matter into account generally fail, because the time-domain EC signal waveform of the same defect can be completely different as shown in Fig. 2.

The abnormal changes of the scanning speed in Fig. 2 (b) were partially caused by resistance to the motion of the EC probe due to a surface crack with abnormal width on the surface and consequently by the reaction of the personnel. In manual scanning, the signal is more affected by noise. These facilities seem to be related to hand motion and the way that the EC probe is held.

These problems were solved by a procedure called Median Signature Tracking [2]. The algorithm is based on non-linear filtering and normalization in the complex plane, instead of time-domain filtering. The analysis consists of the representation of the EC signature as a two-dimensional curve in the complex plane. This approach suppresses the dependence of the signature signal waveform to scanning speed variations. The shape of the EC signature in the impedance plane contains substantial information about the flaw characteristic. The non-linear filtration method was preferred, because it fundamentally provides more abilities to reduce EC signature outliers, the impulse complex noise. Outlier samples are excluded from the output signature and thus from further data processing.

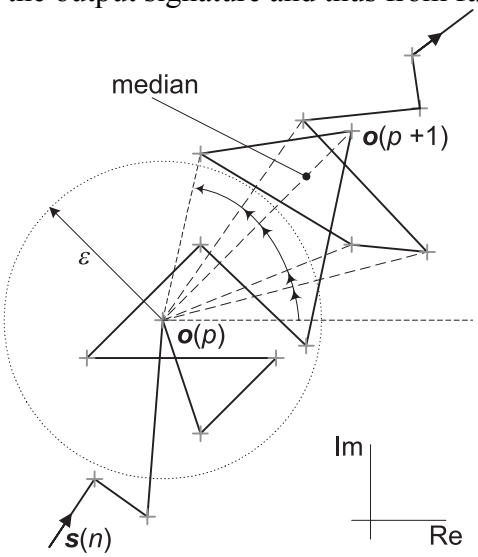

Fig. 3. Median signature tracking algorithm [2]: $\boldsymbol{s}(n)$ is the input noisy signature, $\boldsymbol{o}(p)$ is the output sample from the previous tracking step, and this sample also serves as the origin for the evaluation of sample angles, $\boldsymbol{o}(p+1)$ is the output sample selected via the median of the sample angles, and ε is the size of the circular neighborhood.

The algorithm of the Median Signature Tracking is depicted in Fig. 3. The algorithm measures the distance between consecutive samples in the complex plane, putts away the samples in the close circular neighborhood, and tracks the next sample using a robust estimation of the curvature of the EC signature. The output of the described method represents a down-sampled and filtered version of the input EC signature.

The algorithm is initialized with $k = 1$ for the first sample in the signal segment selected via event detection. A set U of the next M samples with distances greater than ε is composed from the original signal:

$$U = \left\{ \boldsymbol{s}(n) : \left| \boldsymbol{s}(n) - \boldsymbol{o}(p) \right| \geq \varepsilon \wedge n > k \right\}, \tag{5}$$

where $\boldsymbol{s}(n)$ is the input signature, ε is the distance threshold related to the noise level, and p is index of the last output sample.

The local curvature of the EC signature is tracked via the median computed from the angles of the join lines between the individual samples $\boldsymbol{s}(n)$ from the set U and the reference sample $\boldsymbol{o}(p)$. The output sample $\boldsymbol{o}(p+1)$ is chosen as the origin for subsequent sample tracking, and k is updated to the maximum index of the previous set U.

The normalized EC signature, independent of the scanning speed, is then smoothed by anti-causal low-pass filtering converted to the form of a sequence with a constant arc length between samples, and interpolated and re-sampled to a fixed number of samples.

4. Feature Extraction via Modified Fourier Descriptors

Standard Fourier descriptors are based on the expansion of the signature shape in a Fourier series:

$$\boldsymbol{F}(p) = \frac{1}{N}\sum_{n=0}^{N-1} \boldsymbol{s}(n) e^{-j\frac{2\pi}{N}np}, \text{ for } p = 0, 1, 2, ..., (N-1), \tag{6}$$

where $\boldsymbol{s}(n)$ is the EC signature of a length of N samples. For feature extraction, a limited number of coefficients are selected. A classic Fourier descriptor could be used directly for flaw feature extraction or these descriptors can be normalized to describe certain characteristics important for flaw classification such as size, bevel, and depth of a detected flaw and suppress all adverse effects, e.g. offset. The Fourier descriptors were normalized by equations (7) to (9).

$$f_{n1}(r) = \left|\boldsymbol{F}(r)\right| + \left|\boldsymbol{F}(N-r)\right|, \tag{7}$$

$$f_{n2}(r) = \frac{\left|\boldsymbol{F}(r)\right| \cdot \left|\boldsymbol{F}(N-r)\right|}{\max\left(\left|\boldsymbol{F}(r)\right|, \left|\boldsymbol{F}(N-r)\right|\right)^2}, \tag{8}$$

$$f_{n3}(r) = \frac{\arg \boldsymbol{F}(r) + \arg \boldsymbol{F}(N-r)}{2}, \tag{9}$$

where r is the descriptor order, $r \neq 0$. Modified Fourier descriptors f_{n1}, f_{n2}, and f_{n3} correspond to the overall size, ellipticity, and angle of the signature description by harmonic r respectively. There is a possibility to estimate the size (length), bevel, and depth (flaws extending into material). An illustration of the EC signature and its representation by the Modified Fourier descriptor is shown in Fig. 4.

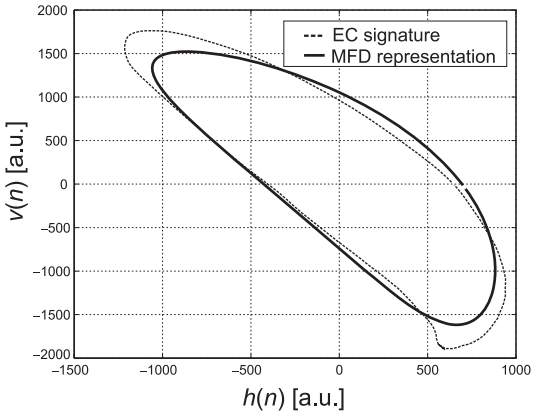

Fig. 4. EC signature representation via Modified Fourier descriptors using the first two descriptor orders

The standard Fourier descriptors characterize the similarity of the EC signature to the complex harmonic function of the frequency. Therefore, the descriptors characterize the EC signature shape in general. There are necessarily many descriptors to enable sufficient

feature extraction for the recognition of flaws and the feature extraction is more susceptible to adverse effects than normalized coefficients, as Modified Fourier descriptors, e.g., offset. A defect must be also characterized by the same representation vector for the two possible scanning directions.

Modified Fourier descriptors were also used for a data processing method enabling a 3D visualization of flaws. This visualization method was implemented into an automated scanning system using motorized eddy current (EC) probe positioning. The three-dimensional image created of a scan result enables the determination of the position of a flaw and the estimation of the size (length) and bevel (angle to surface) of a detected flaw. An example of the visualization of a drilled hole is shown in Fig. 5. The hole was drilled with an angle of 45 degrees and a depth of 20 mm.

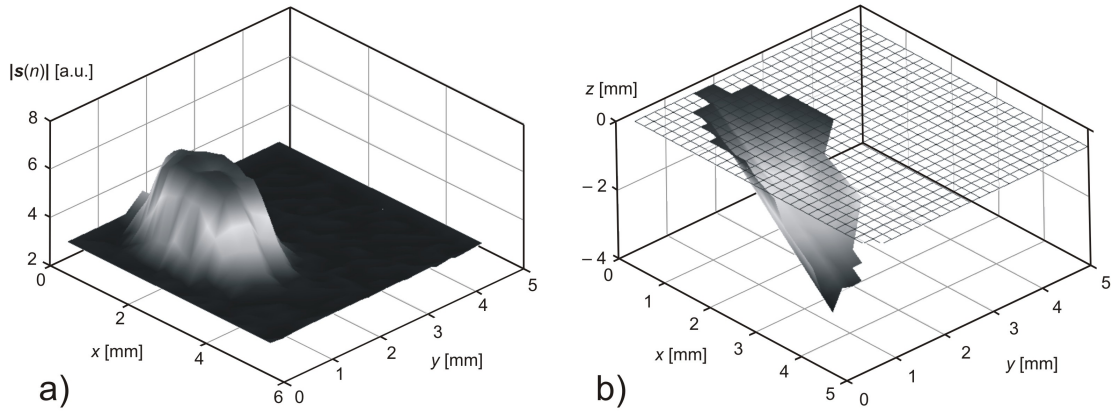

Fig. 5. Visualization of a flaw based on Fourier transformation
(a – absolute value of tester response, b – calculated visualization of the flaw)

5. Classification

The objective of the classification stage is to recognize flaw characteristics such as size, depth, and bevel according to their application-specific severity. In the proposed system, we use a number of classes describing the category of the flaw (e.g. orthogonal flaw with a depth of 0.4 mm). Another approach is to estimate the continuous flaw characteristics via Modified Fourier descriptors (size, angle) using a neural network [2] or a similar method. The classifiers were trained using bootstrapped versions [4] of the training set to improve the learning performance.

5.1 Nearest Mean Classifier

The nearest mean classifier (NMC) assigns input patterns to the nearest class prototype. Each pattern class is represented by a single prototype, which is the mean vector of all the training patterns in that class. The classification function is linear, and thus the decision boundaries are hyper-planes. The Euclidean distance was considered. The NMC is very simple and its classification results are considered to be implementation independent.

5.2 K-Nearest Neighborhood Classifier

The k-nearest neighborhood classifier (KNN) [4] assigns a pattern to the majority class among *k* nearest training patterns. This non-linear classifier requires the computation of the

distances between a test pattern and all the patterns in the training set. In our application we use the Euclidean distance and a value of $k = 4$ neighbors.

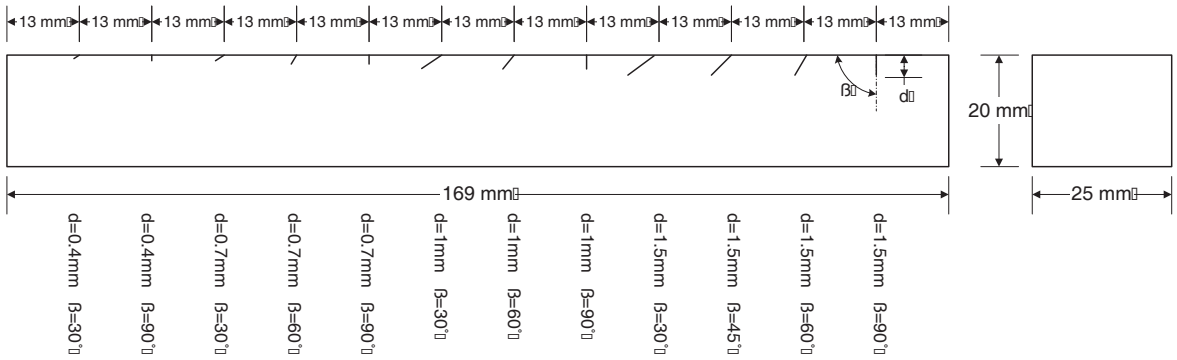

Fig. 6. Tested sample with machined notches (width 0.3 mm, length 25 mm, depth d, angle β)

5.3 Back-Propagation Neural Network

The neural network consists of a number of neurons interconnected via weights, which are iteratively selected during the training of the network [4]. Back-propagation neural networks (BPNN) partition feature space with hyper-planes. We use a network with one hidden layer containing 5–12 neurons (depending on the number of classes) [2]. The network was trained using the back-propagation learning rule with the Levenberg-Marquardt algorithm. This algorithm appears to be one of the fastest methods for training moderate-sized perceptron-based neural networks. The associated class corresponds to the index of the maximum value in the output vector for multi-class classification.

6. Experimental Evaluation

The methods described in the paper were verified on a dataset containing EC signals from the measurement of an aluminum sample. The aluminum sample layout is shown in Fig. 6. The database contains 240 records of notches of a width of 0.3 mm, depths of 0.4, 0.7, 1, and 1.5 mm perpendicular, depths of 0.4, 0.7, 1, and 1.5 mm with an angle of 30°, 0.7, 1, 1.5 mm with an angle of 60°, and 1.5 mm with an angle of 45°. The above-mentioned data was acquired using an absolute shielded probe and a single frequency instrument.

The Median signature tracking method was evaluated by the filtration of artificial noise added to a reference EC signature. The EC signature was measured on an orthogonal notch with a depth of 1.5 mm on the aluminum sample. Two types of noise were added to the signature: an impulse noise and a noise with Gaussian distribution. The noise was admixed separately in each orthogonal direction to the EC signature. The impulse noise was created with amplitude of 1, 2, and 5 % of the signature size in each EC signal component. Similarly, the Gaussian noise was created with a standard deviation value at 1, 2, and 5 % in each direction.

The efficiency of the filtration was evaluated by Signal to Noise Ratio Enhancement (*SNRE*):

$$SNRE = SNR_2 - SNR_1 , \tag{10}$$

where SNR_2 is the signal to noise ratio of the filtered EC signature, and SNR_1 is the signal to noise ratio of the reference EC signature. Similarly to the way that noise was added to the signal, *SNRE* was evaluated in both directions separately. The minimum *SNRE* value from both directions was considered to be the *SNRE* value of the complex filtering procedure.

The comparison of *SNRE* for each kind of noise is shown in Tab. 1. The impulse noise suppression was higher than the suppression of the Gaussian noise. An *SNRE* higher than 20 dB indicates a promising robustness of the procedure. The *SNRE* value for impulse noise with amplitude of 5 % is 63 dB; almost all noise peaks from the output signal were removed. The higher efficiency of impulse noise filtering could be caused by the fact that the noise was added separately to each direction, and thus there was a higher influence of the angles of the join lines between the individual samples $\mathbf{s}(n)$ (chapter 3).

Tab. 1 Evaluation of the Median Signature Tracking Method on Artificial Noise Added to the Signature

Type of noise	Impulse Noise			Gaussian Noise		
Noise Level [%]	1	2	5	1	2	5
SNRE [dB]	26	28	63	16	20	23

The classification performance was evaluated using the bootstrap cross-validation method [4]. The classifier error is estimated as the average error rate on test examples. The estimated error rates are summarized in Tab. 2.

Tab. 2 Classification Performance on the Aluminum Sample, 12 Classes

Classifier	NMC	KNN	BPNN
Error Rate [%]	18.3	10.6	10.1

Conclusion

This paper focused on data preprocessing methods for eddy current inspection, taking into account the effects characteristic for manual EC probe operating as large and unpredictable variations of the scanning speed and alternations of the probe to surface position, e.g. tilt or lift-off. A feature extraction based on the Fourier transformation and following classification via linear classifiers indicate a promising usefulness of data preprocessing methods for the automated analysis of eddy current data during manual inspection.

Acknowledgements

The research work was supported by research program no. MSM 6840770015 "Research of Methods and Systems for the Measurement of Physical Quantities and Measured Data Processing" of the CTU in Prague sponsored by the Ministry of Education, Youth, and Sports of the Czech Republic.

References

[1] Lingvall F, Stepinski T.: Automatic detecting and classifying defects during eddy current inspection of riveted lap-joints. NDT&E Int 2000; 33:47–55.
[2] Šmíd, R., Dočekal, A., Kreidl, M.: Automated Classification of Eddy Current Signatures during Manual Inspection. NDT & International 38 (2005) 462-470, Elsevier Science, 2005.
[3] Oukhellou L, Aknin P.: Modified Fourier descriptors: a new parametrization of eddy current signatures applied to the rail defect classification. In: III International workshop on advances in signal processing for non destructive evaluation of materials, Quebec; 1997, p. 163–9.
[4] Duda R, Hart PE, Stork DG.: Pattern classification. 2nd ed. New York: Wiley, 2001.